WATER FLOW PERFORMANCE OF A SUPERSCALE MODEL OF THE FASTRAC LIQUID OXYGEN PUMP

Stephen Skelley
and
Thomas Zoladz

Fluid Physics and Dynamics Group
Subsystem and Component Development Department
Space Transportation Directorate
Marshall Space Flight Center

ABSTRACT

As part of the National Aeronautics and Space Administration's ongoing effort to lower the cost of access to space, the Marshall Space Flight Center has developed a rocket engine with 60,000 pounds of thrust for use on the Reusable Launch Vehicle technology demonstrator slated for launch in 2000. This gas generator cycle engine, known as the Fastrac engine, uses liquid oxygen and RP-1 for propellants and includes single stage liquid oxygen and RP-1 pumps and a single stage supersonic turbine on a common shaft. The turbopump design effort included the first use and application of new suction capability prediction codes and three-dimensional blade generation codes in an attempt to reduce the turbomachinery design and certification costs typically associated with rocket engine development. To verify the pump's predicted cavitation performance, a water flow test of a superscale model of the Fastrac liquid oxygen pump was conducted to experimentally evaluate the liquid oxygen pump's performance at and around the design point.

The water flow test article replicated the flow path of the Fastrac liquid oxygen pump in a 1.582x scale model, including scaled seal clearances for correct leakage flow at a model operating speed of 5000 revolutions per minute. Flow entered the 3-blade axial-flow inducer, transitioned to a shrouded, 6-blade radial impeller, and discharged into a vaneless radial diffuser and collection volute. The test article included approximately 50 total and static pressure measurement locations as well as flush-mounted, high frequency pressure transducers for complete mapping of the pressure environment. The primary objectives of the water flow test were to measure the steady-state and dynamic pressure environment of the liquid oxygen pump versus flow coefficient, suction specific speed, and back face leakage flow rate. Initial results showed acceptable correlation between the predicted and experimentally measured pump head rise at low suction specific speeds. Likewise, only small circumferential variations in steady-state impeller exit and radial diffuser pressure distributions were observed from 80% to 120% of the design flow coefficient, matching the computational predictions and confirming that the integrated design approach has minimized any exit volute-induced distortions. The test article exhibited suction performance trends typically observed in inducer designs with virtually constant head rise with decreasing inlet pressure until complete pump head breakdown. Unfortunately, the net positive suction head at 3% head fall-off occurred far below that predicted at all tested flow coefficients, resulting in a negative net positive suction head margin at the design point in water. Additional testing to map the unsteady pressure environment was conducted and cavitation-induced flow disturbances at the inducer inlet were observed. Two distinct disturbances were identified, one rotating and one stationary relative to the fixed frame of reference, while the transition from one regime to the next produced significant effects on the steady state pump performance. The impact of the unsteady phenomena and the corresponding energy losses on the unexpectedly poor pump performance is also discussed.

INTRODUCTION

Marshall Space Flight Center (MSFC) has developed a 60,000 pound thrust rocket engine for use on the Reusable Launch Vehicle Technology Demonstrator vehicle (X-34). The gas generator cycle engine, also called the Fastrac engine, uses liquid oxygen and RP-1 for propellant. The turbopump integrates a single stage liquid oxygen pump, a single stage RP-1 pump, and single stage supersonic turbine into a compact assembly on a common shaft. A cross section of the turbopump appears in figure 1.

Figure 1. Fastrac Turbopump Cross Section

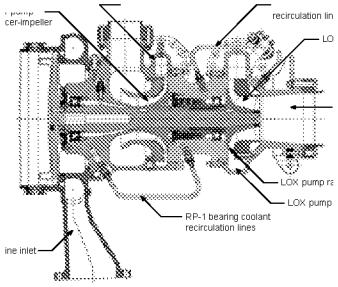

The engine was designed entirely by MSFC personnel and the turbopump design included the first use and application of new suction capability prediction methods and three-dimensional blade generation codes. In response to previous experiences with liquid oxygen pumps, a water flow test to evaluate the suction capability and head performance of the liquid oxygen pump was proposed. Using a superscale model of the pump, a test was conducted in MSFC's Inducer Test Loop during the first half of 1999 to evaluate the test article performance at scaled operating conditions in water. This document is intended to summarize the results from the experimental water flow test.

TEST FACILITY DESCRIPTION

The Inducer Test Loop is a closed loop water flow test facility with manual set point control of flow rate, shaft speed, water temperature, and test article inlet pressure. In operation flow leaves the 300 gallon stainless steel reservoir through an 8 inch line, transitions to 6 inch line, passes through a flow straightener section, and enters the test article. High pressure discharge flow exits the test article, passes through a 6 inch turbine type flow meter, and returns to the reservoir. A 6 inch quiet valve provides remote back pressure control for flow rate adjustment. Test article inlet pressure is controlled by pressurizing or evacuating the small air volume at the top of the reservoir. This reservoir ullage pressure, coupled with the line losses between the reservoir and test article inlet and the height of the water in the reservoir itself, is used to set a wide range of inlet pressures - from 165 down to 3 pounds per square inch absolute. The test loop accommodates flow rates up to 4000 gallons per minute and is constructed primarily of schedule 40 and schedule 80 PVC. An auxiliary loop removes dissolved air from the test fluid and maintains water temperatures between 70 and 100 degrees Fahrenheit. The driveline consists of a 3-phase, 150 horsepower motor with a variable speed controller and belt driven bearing box. Design limit speed is approximately 6000 revolutions per minute, but higher speeds are obtainable by changing the pulley ratio and belt material. Bearing temperatures, shaft speed, test article inlet pressure, flow rate, water temperature, and discharge pressure are monitored at the facility operator's control panel and an Orbiscope dissolved oxygen sensor is used to measure the water dissolved oxygen content. For all testing water dissolved oxygen content was maintained at or below 4 parts per million.

TEST ARTICLE DESCRIPTION

The test article was a superscale (1.582X) model of the Fastrac liquid oxygen pump and replicated the primary flow path including the front and rear leakage cavities. Bearing coolant flow, or back face leakage, was collected metered, and returned to the pump inlet through 2 external lines. A cross section and front view of the test article appears in figure 2.

Figure 2. Test Article Cross Section and Front View

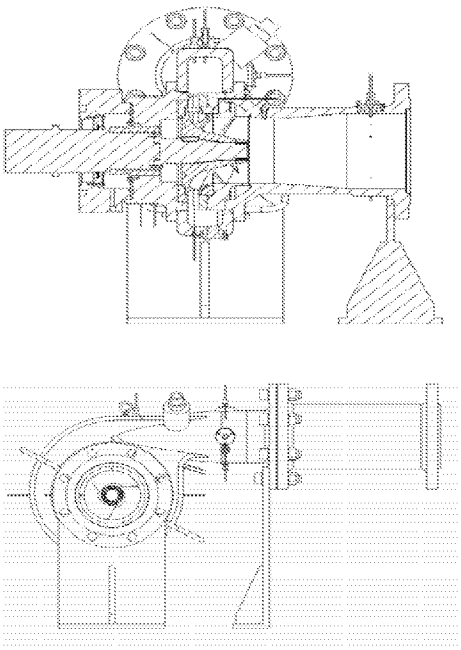

The stainless steel inducer-impeller shown in figure 3 was fabricated by Turbocam, Inc. and included 3 full length blades and 3 splitters, resulting in 6 shrouded flow passages at the impeller discharge. No back face pumping vanes were included on the test article inducer-impeller although the prototype includes this design feature. The stainless steel inducer-impeller was a replacement for the original aluminum inducer-impeller which was damaged after approximately 20 hours of testing. High cycle fatigue resulted in the loss of the tips of each of the 3 inducer blades. The

steel inducer-impeller suffered no fatigue or cavitation-induced damage during testing.

Figure 3. Inducer-Impeller Assembly

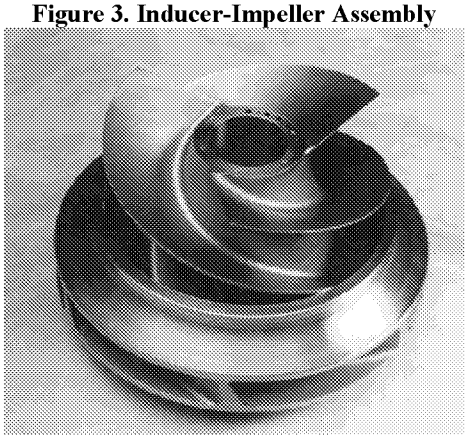

Impeller discharge flow was guided through a vaneless, constant width radial diffuser, rectangular cross section volute, and conical exit diffuser and directed away from the pump perpendicular to the axis of rotation. Table 1 summarizes the scaled and as-built geometric parameters for the test article. Table 2 summarizes the prototype and test article design point operating conditions.

Table 1. Test Article Geometric Parameters

Number of Blades	3 + 6
Inlet Tip Diameter	5.177 inch
Inlet Hub Diameter	1.973 inch
Reference Blade Length (Hub to Tip)	1.736 inch
Leading Edge Tip Thickness	0.019 inch
Inlet Blade Angle at Tip	10.5 degrees
Inducer Radial Clearance	0.021 inch
Exit Tip Diameter	7.056 inch
Exit Blade Height	0.682 inch
Exit Blade Angle	26.5 degrees
Radial Diffuser Inner Diameter	7.147 inch
Radial Diffuser Outer Diameter	9.487 inch
Radial Diffuser Passage Width	0.684 inch
Volute Throat Area	6.660 sq inch
Exit Diffuser Cone Angle	6.00 degrees
Exit Diffuser Cone Length-to-Inlet Radius Ratio	5.00
Exit Diffuser Cone Exit Diameter	4.182 inch

Table 2. Prototype and Test Article Design Point

Parameter	Prototype	Test Article
Fluid	Liquid Oxygen	Water
Fluid Temperature	166 deg R	90 deg F
Shaft Speed	20,000 rpm	5000 rpm
Inlet Flange Flow Rate	880.4 gpm	870 gpm
Impeller Flow Rate	923.7 gpm	913 gpm
Inlet Flange Total Pressure	46.0 psia	4.7 psia
Back Face Leakage Rate	25.6 gpm	25.3 gpm
Net Positive Suction Head	59.2 ft	9.2 ft
Inlet Tip Flow Coefficient	0.135	0.135
Suction Specific Speed (rpm, gpm, ft)	27820	27820

All test article hardware except the inducer-impeller was fabricated of anodized 2219 aluminum by Dynamic Engineering, Inc. The test article design inlet pressure, shaft speed, and discharge pressure were 40 pounds per square inch absolute, 6000 revolutions per minute, and 165 pounds per square inch absolute, respectively.

INSTRUMENTATION

Steady-state measurements acquired during testing were used to confirm set point conditions, evaluate pump performance, and monitor test article health. Surface static pressure taps were distributed throughout the test article and grouped into 12 axial measurement planes. Total pressure probes at the inlet and discharge flanges were used to establish flange-to-flange pressure rise and a flow direction probe at the impeller discharge further defined pump performance. Flush-mounted high frequency response transducers were also located at 3 axial planes in the test article and at 4 locations in the facility piping for recording of system and pump pressure oscillations. Accelerometers on the test article were used to resolve motion of the stationary components. The approximate locations, types, and numbers of these measurements appear in figure 4.

Figure 4. Test Article Measurement Locations, Types, and Numbers

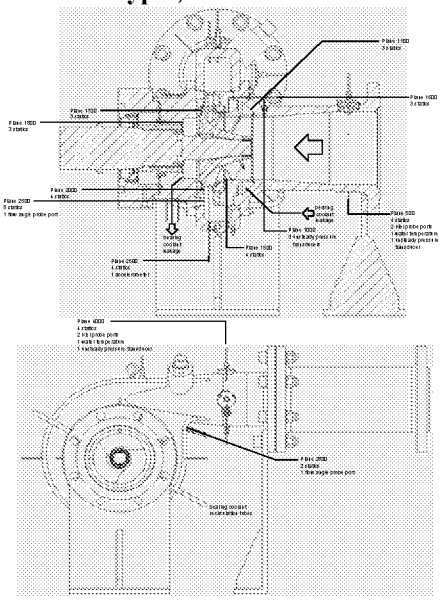

TEST PLAN

The objectives of the experimental water flow test were to

1. Measure the steady-state pump suction performance versus flow coefficient and back face leakage flow rate.
2. Measure the pump steady-state head performance versus flow coefficient and back face leakage flow rate.
3. Measure the pump dynamic pressure environment versus flow coefficient, suction specific speed, and back face leakage flow rate.
4. Measure pump intra-stage pressures for verification of design code predictions.

An implied objective was to provide a safe and inexpensive test article to support potential failure investigations or redesign efforts. The original test plan included pump operation as low as 50% of the design flow coefficient. Following the failure of the aluminum inducer-impeller, all testing and operation with the replacement steel inducer-impeller was confined to a range of 80% to 120% of the design flow coefficient. Likewise, the installed back face leakage routing lines included too much resistance, so operation with higher than the nominal scaled leakage flow rate was not possible. Test variables included flow coefficient, suction specific speed, and back face leakage flow rate. The test article set point variables were then water temperature, inlet flange flow rate, inlet flange total pressure, shaft speed, and back face leakage rate. The as-tested ranges of each of the test variables appear in table 3 for a shaft speed of 5000 revolutions per minute.

Table 3. Completed Test Matrix

Back Face Leakage Rate	Percent Design Flow Coefficient	Suction Specific Speed
Nominal	80%	6340 - 29010
	90%	5670 - 28680
	100%	5550 - 27580
	110%	5780 - 26260
	120%	5770 - 25170
Half Nominal	90%	8030 - 24560
	100%	5660 - 26000
	110%	7530 - 24700
Zero	90%	7820 - 28200
	100%	7470 - 27830
	110%	8030 - 26620

STEADY STATE PERFORMANCE

The overall stage total and static pressure rise as well as the total and static pressure rise of the inducer-impeller appear in figure 5 versus percent design flow coefficient. Pressure rise data in figure 5 are values corresponding to a suction specific speed at or below 10000 for the nominal back face leakage flow rate. Data has been non-dimensionalized by the impeller tip speed and the predicted performance curve included for reference. The trends are as expected with steadily decreasing pressure rise with increasing flow rate. The water flow test article appeared to underperform slightly at and below the design flow coefficient with head rise at the higher flow rates much closer to the predicted. Expressed in terms of degree of reaction, or the ratio of impeller static head rise to stage total head rise, the experimental value at the design flow coefficient was 0.83, indicating excellent conversion of available dynamic head to static pressure.

Figure 5. Stage and Inducer-Impeller Head Coefficient versus Percent Design Flow Coefficient

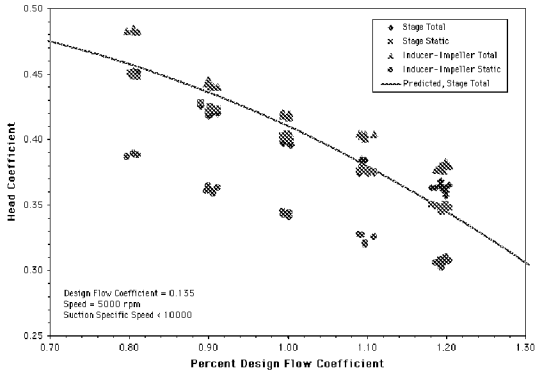

The experimental pump stage suction performance appears in figure 6 with stage head coefficient versus inlet flange suction specific speed. The individual curves correspond to flow coefficients from 80% to 120% of the design flow coefficient. The trends are as expected with inducer-impeller designs with virtually constant head coefficient with decreasing inlet pressure. The small reduction in steady state head rise at a suction specific speed of approximately 17000 to 21000 was attributed to the transition of a rotating, cavitation disturbance at the inlet to a synchronous, uniform cavity oscillation. Complete head breakdown soon follows. The approximate range of the inlet rotating disturbance was from a suction specific speed of 11500 to 17000 and further discussion of the observed unsteady phenomena appears in a later section. The pump design point and calculated 3% head loss curve are included for reference. As this curve illustrates, the test article failed to achieve the desired suction performance in water at the design flow coefficient with a calculated margin on net positive suction head of –9% between the demonstrated and required capability. The measured variation in head coefficient at the 110% design flow coefficient was attributed to electrical contamination of the stage pressure rise measurement during those set points. All other data included in this document remained unaffected.

Figure 6. Stage Head Coefficient versus Suction Specific Speed and Percent Design Flow Coefficient

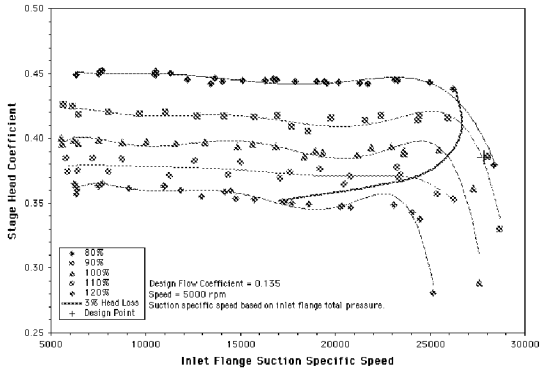

For comparison the inducer-impeller head coefficient is plotted versus suction specific speed and percent design flow coefficient in figure 7. No variation is observed in the 110% design flow coefficient data.

Figure 7. Inducer-Impeller Head Coefficient versus Suction Specific Speed and Percent Design flow Coefficient

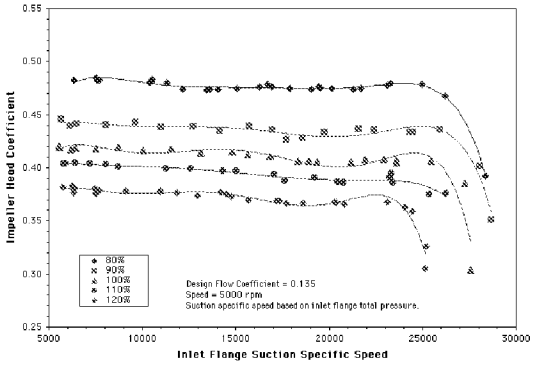

A primary design objective was to minimize the impeller discharge distortion and thereby minimize the fluid-induced pump sideloads. Figure 8 shows the measured static pressure distribution at the impeller discharge versus percent design flow coefficient. A view slightly further downstream appears in figure 9 with the static pressure distribution at the exit of the radial diffuser. Each location shows increasing influence of the volute cutwater – located at 24 degrees – with the least pressure variation at each location at the design flow coefficient. In each plot the static pressure coefficient is defined as the local pressure divided by the plane average static pressure and divided by the calculated dynamic pressure.

Figure 8. Static Pressure Distribution at the Impeller Discharge

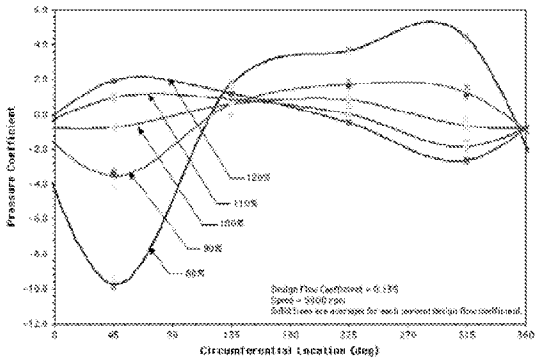

Figure 9. Static Pressure Distribution at the Radial Diffuser Discharge

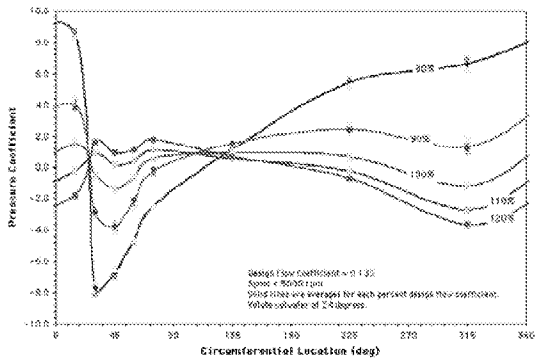

The final check on inducer-impeller performance was via a single flow direction probe located slightly downstream of the impeller discharge in the center of the radial diffuser. Total pressure, static pressure, and probe-relative flow angle was then derived from the sensed pressures and the probe calibration results. The impeller discharge flow angle relative to impeller tangential versus percent design flow coefficient appears in figure 10. The predicted discharge flow angle at the design flow coefficient was 14 degrees relative to impeller tangential.

Figure 10. Impeller Discharge Flow Angle versus Percent Design Flow Coefficient

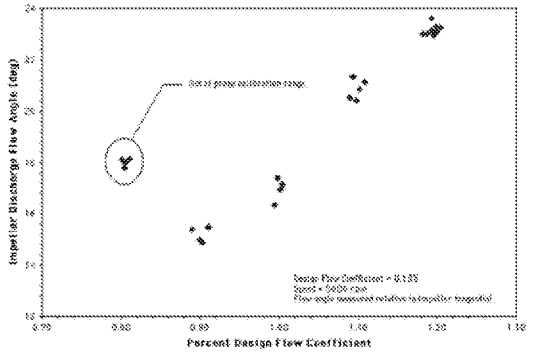

The majority of data was collected at a back face leakage rate corresponding to the nominal condition. However, limited performance data was collected at half the nominal leakage rate and with the external leakage metering lines closed. The effect of reducing the leakage rate on stage head rise appears in figure 11 for suction specific speeds at or less than 10000. As expected the stage head rise increases with decreasing leakage rate as work previously expended on the leakage flow is applied to the throughflow. The inducer actually operates at a slightly lower flow coefficient as the leakage flow is reduced at constant pump flow rate and thereby contributes a small amount to the increase in stage performance.

Figure 11. Stage Head Coefficient versus Percent Design Flow Coefficient and Leakage Rate

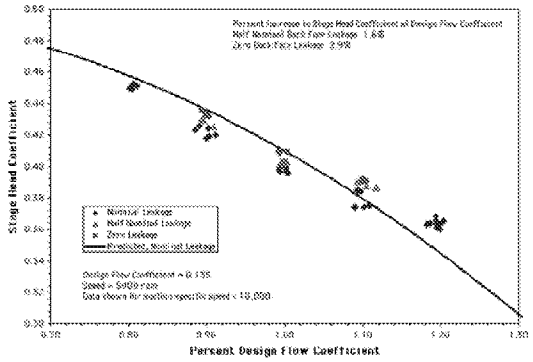

Although a small effect on suction performance appears in the leakage rate comparison in figure 12, the calculated differences are of the same order as the experimental uncertainty at these values of suction specific speed. No conclusion should then be drawn from these results. Figure 11 is then included to illustrate the repeatability of the small drop in stage performance, which appears for each configuration near a suction specific speed of 17000. This performance drop, as will be seen in the following section, corresponds to the highest amplitude of the synchronous cavity oscillation at the inducer inlet.

Figure 12. Stage Head Coefficient versus Suction Specific Speed and Leakage Rate at Design Flow Coefficient

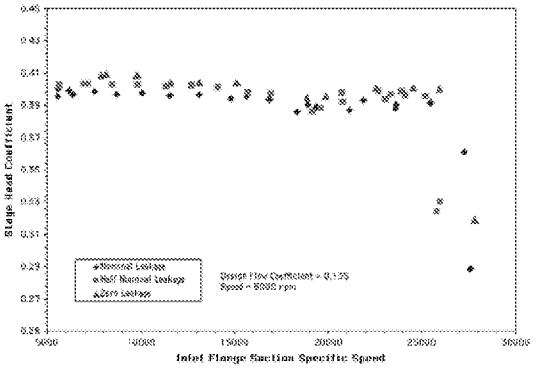

UNSTEADY PERFORMANCE

Figure 13 shows the progression of unsteady oscillations versus time as the pump inlet pressure was steadily reduced at a constant shaft speed of 5000 revolutions per minute (83.3 Hertz) at the design flow coefficient. At low suction specific speeds, the oscillation at 3 times shaft speed (3N)

was most prominent as was associated with the wakes from the 3 inducer blades. As suction specific speed approached 11000 at 88.5 seconds the 3N oscillation transitioned to a rotating disturbance moving at approximately 1.2 times the shaft speed (1.2N) as viewed from a stationary observer. This rotating disturbance was identified as a single cavitation cell moving opposite the direction of shaft rotation. Further reduction in inlet pressure causes the single-cell rotating disturbance to transition to a stationary oscillation with a frequency equal to the shaft speed. Simultaneously a higher amplitude oscillation appeared with a frequency very close to the fundamental frequency of the test facility piping – approximately 10 Hertz. These low frequency and synchronous oscillations persisted as inlet pressure was reduced and head breakdown was reached. The potential for dynamic coupling between the facility and pump was recognized and attempts were made to better isolate the pump from the facility. All were unsuccessful and the low frequency oscillation appeared to "lock-in" with the facility harmonic at all tested flow coefficients.

Figure 13. Oscillation Amplitudes versus Frequency and Time at Constant Speed and Design Flow Coefficient

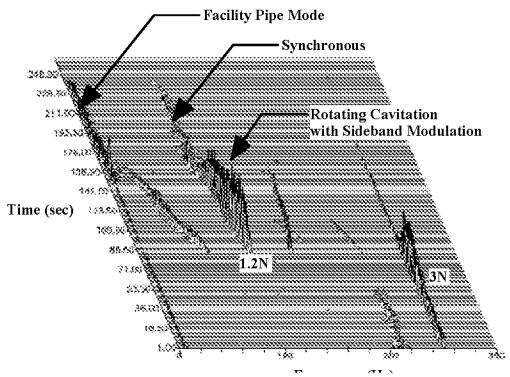

The dynamic coupling between the test article and facility, combined with the presence of cavitation, suggested the occurrence of auto-oscillation, if only for a brief period. Brennen[1] noted severe steady state performance deficits due to the energy dissipation during auto-oscillation and the magnitude of the head loss at the design flow coefficient was approximately 3%. The nondimensional amplitudes of the oscillations noted in figure 13 and stage head coefficient appear in figure 14 versus suction specific speed. Oscillation amplitudes have been normalized by the dynamic pressure based on impeller tip speed while head coefficient has been normalized by the non-cavitated value. For comparison the corresponding normalized amplitudes from recent component testing in liquid oxygen are included.

Figure 14. Oscillation Amplitudes versus Suction Specific Speed

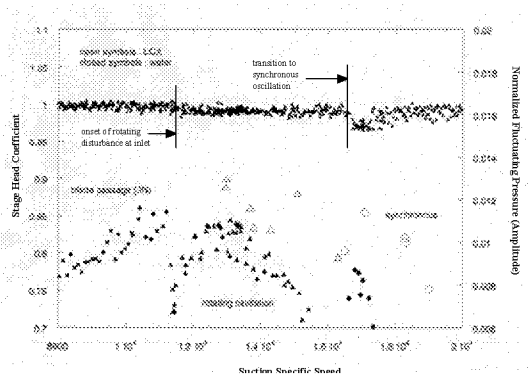

Auto-oscillation is typically characterized by high amplitude, system-wide oscillations in pressure and flow rate. As seen in figure 13, pressure oscillations during auto-oscillation were highest at the onset of the phenomena. These oscillations appeared in conjunction with noticeable facility piping displacements and low frequency, shock-like vibrations. However, the period of these high intensity vibrations and pressure oscillations was brief and occupied only a very narrow band of suction specific speed values. The relationship between the synchronous oscillation and the appearance of auto-oscillation is still under review, but the transition of a rotating cavitation disturbance to a fixed number of cavitation cells oscillating in unison has been observed in other inducer performance investigations. Rosenmann[2] and others[3,4] observed the transition of a rotating disturbance to a "unidirectional" or synchronous oscillations with frequency equal to the shaft speed just before head breakdown. The relationship between the uniform cavity or synchronous oscillation and the corresponding system dynamic response and the subsequent onset of auto-oscillation requires further investigation. Regardless, the pump and system dynamic interaction appears to have contributed to the inability of the test article to achieve the expected suction capability. Although beyond the scope of this document, the significance of the data in figure 14 for the prototype pump operating in liquid oxygen should be noted. Despite the difference in test facility configurations, the prototype exhibited similar unsteady performance characteristics with the appearance of a synchronous oscillation at high suction specific speeds. This may

suggest a sensitivity of the pump to dynamic system interactions.

UNCERTAINTY ANALYSIS

An uncertainty analysis incorporating the experimental precision and bias errors using the root-sum-square method was performed to quantify the worst case uncertainties associated with the measured and calculated quantities. A 95% confidence level was assumed. The estimated uncertainties for each of the parameters presented here are summarized in table 4. Since the estimated uncertainty associated with suction specific speed is a dominated by the nonlinear function of pressure, the quoted uncertainty for suction specific speed in table 4 corresponds to a suction specific speed of 27000.

Table 4. Estimated Uncertainties

Parameter	Uncertainty
Stage Head Coefficient	± 0.005
Impeller Head Coefficient	± 0.007
Percent Design Flow Coefficient	± 0.05
Suction Specific Speed	± 800
Pressure Coefficient	± 0.04
Impeller Discharge Flow Angle	± 1.2 degree

CONCLUSIONS

Although this document is intended to merely summarize the experimental performance of the superscale water flow test, a few general conclusions regarding the Fastrac liquid oxygen pump performance can be made:

1. Steady state stage head rise was lower than predicted for 80% to 100% of the design flow coefficient. At 120% of the design flow coefficient, steady state stage head rise exceeded the predicted performance.
2. Suction performance in water failed to meet the desired capability with a margin on net positive suction head of –9%.
3. Three regimes of unsteady oscillations were observed, identified, and tracked versus pump operating parameters, including a brief period of auto-oscillation.
4. The appearance of auto-oscillation corresponded to drops in the steady state stage head rise of approximately 3% at the design flow coefficient.
5. The onset of auto-oscillation was unaffected by reduction in the pump back face leakage flow rate.

ACKNOWLEDGEMENTS

The authors gratefully acknowledge Jeff Moore and Teddy Stephens of the Experimental Fluid Dynamics Group for their operation of the experimental test facility and assistance with test article and instrumentation installation. The measurement systems were designed, integrated, and maintained by Drew Smith and Herb Bush, also of the Experimental Fluid Dynamics Group. Richard Branick of Sverdrup was responsible for test article assembly. The authors would also like to recognize Stephen Fritz of Cortez III for his incredible electrical troubleshooting skills.

REFERENCES

[1] Brennen, C. E., Hydrodynamics of Pumps, Concepts ETI, Inc. and Oxford University Press, Norwich, 1994.

[2] Rosenmann, W., "Experimental Investigation of Hydrodynamically Induced Shaft Forces with a Three Bladed Inducer," Symposium on Cavitation in Fluid Machinery, ASME Winter Annual Meeting, Chicago, IL, Nov. 7-11, 1965.

[3] Kamijo, K., Yoshida, M., and Tsujimoto, Y., "Hydraulic and Mechanical Performance of LE-7 LOX Pump Inducer," Journal of Propulsion and Power, vol. 9, no. 6, 819-826, 1993.

[4] Kamijo, K., Shimura, T., and Watanabe, M., "A Visual Observation of Cavitating Inducer Instability," National Aerospace Lab (Japan) Report NAL TR-598T, 1980.